


Purification and the effects on structure and bioactivity for polysaccharide from *Actinidia valvata* Dunn. using macroporous adsorption resin

Feng PAN^{1,2#}, Sanhua LI[#], Xinting ZHU², Jianbo YANG³, Jing WEN¹, Changwei SONG¹, Xirong LUO⁴, Guoyong RUAN^{3*}, Yun LIU^{1,2*} 

Abstract

Resin AB-8 was screened from seven resins with different polarity and particle size because of its better decoloration and deproteinization efficiency to polysaccharide from the root of *Actinidia valvata* (AvPs), and then the optimized parameter conditions were applied by the single-factor experiments and were shown as follows: a concentration of crude polysaccharide of 3 mg/mL, an adsorption time of 40 min, an initial pH of 7.0, a flow rate of 1.5 BV/h. In addition, the results of HPGPC, FT-IR, PMP-HPLC-DAD, ¹H NMR and Congo red test showed that the sugar chain, structural group, monosaccharide composition and triple-helix conformation structure of AvPs were not broken during resin AB-8 treatment. Moreover, AvPs could keep the stability of biological activity after the resin AB-8 treatment, and revealed an obviously antioxidant and anticancer activities *in vitro* as well. This research suggests that this method is promising for the deproteinization and decolorization of AvPs which could be explored as a potential antioxidant or anticancer agent for use in functional food or medicine.

Keywords: macroporous resin; decoloration; deproteinization; antioxidant and anticancer activities; polysaccharide from *Actinidia valvata* dunn.

Practical Application: Purification and the effects on structure and bioactivity for polysaccharide from *Actinidia valvata* Dunn. using macroporous adsorption resin.

1 Introduction

The genus *Actinidia* (family Actinidaceae) includes nearly sixty species, and some of them are well known worldwide for their delicious kiwi fruits, and some of them are used as herbal medicines because of a significant clinical effect on some diseases for a long time in China (Xiao et al., 2014). *A. valvata* Dunn. affiliated to the genus *Actinidia*, family Actinidaceae. The root of *A. valvata* Dunn. which is a shrub mainly growing in eastern China, is known as “mao ren shen” in traditional Chinese medicine, exhibits antitumor, anti-inflammatory activity, antioxidant activity, immune boosting, and is being increasingly used to treat a wide variety of clinical diseases, such as gastric cancer, esophagus cancer, hepatoma, lung carcinoma and myeloma (Feng et al., 2004; Wang et al. 2005; Xin et al., 2008; Zhang et al., 2006).

Active components from medicinal herbs are effective for research and development of new drugs (Jamshidi-Kia et al., 2018). Polysaccharides, biological macromolecules, have a variety of biological activities, such as antioxidant, antitumor, immunoregulatory and anti-inflammatory activities without toxicity (Braunlich et al., 2018; Carnachan et al., 2019; Li et al., 2020; Liu & Li, 2020; Yu et al., 2018). Previous researches had shown that polysaccharides, as macromolecular compounds, from the roots of the genus *Actinidia* had antitumor activity,

which might contribute to the clinical effect of antitumor. For example, polysaccharide from *A. chinensis* planch could protect against hypoxia-induced apoptosis of cardiomyocytes *in vitro* (Wang et al., 2018). And the polysaccharide from the roots of *A. eriantha*, could activate RAW264.7 macrophages via TLRs/NF- κ B signaling (Sun et al., 2015), and might induce macrophage activation through regulating miRNAs expression (Chen et al., 2019). However, ignorance of macromolecular chemical constituents of *A. valvata*, although their effect on cancer has been shown by long clinical experience, hampered its further study and more widespread agreement (Xu et al., 2009). Therefore, the polysaccharides were extracted from the root of *A. valvata* (AvPs) and found that the crude polysaccharides contained many impurities such as proteins and pigments.

Decoloration and deproteinization are necessary for purification of AvPs since excessive impurities make the further application of AvPs in pharmaceutical industry and other relevant industries more difficult, and colored impurities also cause severe pollution of Sephadex Gel during further purification, resulting in high operating cost and interference in structural and functional detection (Liang et al., 2019). The conventional methods for decoloration, such as hydrogen peroxide, activated carbon adsorption, are applied in laboratories and experiments

Received 29 Sept., 2021

Accepted 02 Nov., 2021

¹Institute of Life Sciences, Zunyi Medical University, Zunyi, Guizhou, China

²Department of Biochemistry and Molecular Biology, Zunyi Medical University, Zunyi, Guizhou, China

³Guizhou Guangzheng Pharmaceutical, Guiyang, Guizhou, China

⁴Department of Modern Agriculture, Zunyi Vocational and Technical College, Zunyi, Guizhou, China

*Corresponding author: liuyunzmu@126.com, 625620202@qq.com

#The first two authors contributed equally to this work

in food or pharmaceutical industry (Jia et al., 2013; Xie et al., 2011). However, the low selectivity coefficient (Agudo et al., 2002), high operation costs (Li et al., 2012), and changes of biological activity (Yang et al., 2012) of those methods limit its application in decoloration of AvPs. In addition, multiple methods, such as Sevag method, the trichloroacetic acid method, sodium chloride method, freeze-thaw treatment, proteases method and part of these methods combined method, have been used for deproteinization from crude polysaccharides (Huang et al., 2012; Pan et al., 2018; Sevag et al., 1938; Xing et al., 2013). However, the deficiencies of these methods still limit their application for most industrial applications. For example, the Sevag method consumes a large amount of toxic organic reagents, and leads to residual toxic organic reagents in the product (Shi et al., 2019), and the freeze-thaw method takes a long time, and consumes a lot of electricity to obtain pure polysaccharides (Shi et al., 2019). The trichloroacetic acid method can result in the partial hydrolysis of polysaccharide (Liu et al., 2010). Therefore, a safe and efficient method of decoloration and deproteinization of AvPs is indispensable. Macroporous resin has double functions of simultaneous decoloration and deproteinization under moderate and environmentally friendly conditions. Up to now, macroporous resin adsorption was used to simultaneously remove proteins and pigments in polysaccharides extracted from several plants, such as *Solanum nigrum* L. (Huang et al., 2021); *Typha angustifolia* (Shi et al., 2019), *Cucurbita moschata* Duch (Liang et al., 2019), because of the simpler procedure, less labour intensity, lower yielding cost, easier scale-up and high security. Therefore, in the present report, macroporous resin adsorption as a new method was used to develop for the deproteinization and decolorization of crude AvPs.

2 Materials and method

2.1 Materials and reagents

The roots of *Actinidia valvata* Dunn. were collected in Qizhou Medicinal Materials Market in Anguo City, Hebei Province, P. R. China, in October 2018. The sample was dried at 60 °C, and ground into a powder.

Macroporous resins (Types: S-8, X-5, HP-20, AB-8, D101, HPD100, DM301) were provided by Donghong Chemical Co., Ltd., (Shandong, China). Standard monosaccharides with a purity of at least 97% (D-(+)-mannose, D-ribose, L-rhamnose, D-(+)-glucose, D-(+)-galactose, L-(+)-arabinose and L-(-)-fucose) were purchased from BioDuly (Nanjing, China). 2,2-azino-bis(3-ethylbenzthiazoline-6-sulfonic acid) (ABTS) was purchased from Sigma-Aldrich (Shanghai, China). Congo red (>98.0% purity, HPLC) was purchased from Aladdin (Shanghai, China). All other chemicals and solvents were of analytical reagent grade.

2.2 General experimental procedures

pH value of the diluted molasses was measured by pH meter (pH 700, Eutech Instruments, Singapore) fitted with a temperature compensator. The desorption/regeneration of resins was performed using 5% HCl, followed by washing with water to remove the residual HCl, and then performed using 5% NaOH with the similar process. Those resins were dried with absorbent

paper before using. Aqueous solution was concentrated by rotary evaporation (EYELA N-1300, Shanghai Eyela Instrument Co., Ltd., Shanghai, China). Centrifugation of polysaccharide samples was performed on an HDL-40B centrifuge system (Changzhou Hongke Instrument Factory, China). Polysaccharides are dried on a Telstar LyoQuest freeze drier (Azbil Telstar Technologies SLU, Spain). The absorbance (Abs) was measured on a SpectraMax® i3x fluorescence microplate reader (MOLECULAR DEVICES) using 96-well plate method, and the wavelength was selected according to experimental needs.

2.3 Extraction of crude polysaccharide.

The powder of *A. valvata* Dunn root was ultrasonically extracted using 95% ethanol (EtOH) with a material-liquid ratio of 1:10 (g/mL) for 2 h for three times. The filtered residue was extracted using pure hot water (80±2 °C) with a material-liquid ratio of 1:30 for 2 h. After filtering with 4 layers of gauze, the filtrate was collected and concentrated to quarter of its original volume, followed by soaking in 80% ethanol for overnight at 4 °C. The precipitation (crude polysaccharide) was centrifuged, dried, collected, weighed and named crude AvPs.

2.4 Analytical methods

Determination of decoloration ratio

The decoloration ratio was measured using the method described by Liang and Wang (Liang et al., 2019; Wang et al., 2012). In short, the absorbance (Abs) of polysaccharide solution was determined at 420 nm. The decoloration ratio (Dcr%) of crude polysaccharide treated by the resins was calculated as follows in Equation 1:

$$\text{the decoloration ratio (Dcr\%)} = \frac{(A_{C0} - A_{C1})}{A_{C0}} \times 100\% \quad (1)$$

where A_{C0} and A_{C1} were the Abs of the sample solutions at 420 nm before and after decoloration using resins, respectively. All experiments were performed in triplicate.

Determination of deproteinization ratio

The protein content was determined using the Bicinchoninic acid (BCA) assay as described by Walker (2009). And the deproteinization ratio was calculated as follows in Equation 2:

$$\text{the deproteinization ratio (Dpr\%)} = \frac{(A_{p0} - A_{p1})}{A_{p0}} \times 100\% \quad (2)$$

where A_{p0} and A_{p1} were the Abs values of the sample solutions before and after deproteinization using resins, respectively. All experiments were performed in triplicate.

Determination of recovery ratio

The content of carbohydrate in solution was determined by the previously reported phenol-sulfuric acid method (Masuko et al., 2005) with some modifications, and using glucose as a reference.

Sample solution (100 μL) was mixed with 200 μL 5% phenol solution, then 1.0 mL sulfuric acid was added and hold for 5 min at 95 $^{\circ}\text{C}$. 100 μL post-reaction solution was transferred to the 96-well microplate and measured at 490 nm. The recovery ratio ($R_{rr}\%$) was calculated as follows in Equation 3:

$$\text{the recovery ratio (Rrr\%)} = \frac{A_{r1}}{A_{r0}} \times 100\% \quad (3)$$

where A_{r0} and A_{r1} were the Abs values of the sample solutions before and after adsorption using resins, respectively. All experiments were performed in triplicate.

Comprehensive adsorption effect index (ξ)

The weighted sum of $D_{cr}\%$, $D_{pr}\%$ and $R_{rr}\%$ was calculated to represent the comprehensive adsorption effect index ξ ($0 \leq \xi \leq 1$) (Shi et al., 2019). A larger value of ξ indicates a better comprehensive adsorption effect. The value of ξ was calculated as follows in Equation 4:

$$\xi_i = \sum_{j=1}^3 (X_{ij} \times W_j); j=1,2,3, \quad (4)$$

Where X_{ij} corresponded to the $D_{cr}\%$ ($j=1$), $D_{pr}\%$ ($j=2$) and $R_{rr}\%$ ($j=3$), and W_j corresponded to the weights of $D_{cr}\%$ ($j=1$), $D_{pr}\%$ ($j=2$) and $R_{rr}\%$ ($j=3$). And the values of W_1 , W_2 and W_3 were set to 0.3, 0.3 and 0.4, respectively, due to $R_{rr}\%$ with the most important index in this work, as the described by Shi et al. (2019). All experiments were performed in triplicate.

2.5 Optimization of resin types and adsorption conditions by static adsorption

To screen the best resin types and processing parameters, the effects of adsorption time, the concentration and initial pH of AvPs solution were investigated using single-factor experiments. The value of ξ served as the indicator of adsorption. All experiments were performed in triplicate.

Resin types

Static adsorption tests of polysaccharides using different resins with different polarity and particle size (S-8, X-5, HP-20, AB-8, D101, HPD100 and DM301) were performed. In each time, 2 g of pretreated resins and 20 mL of crude polysaccharide solution (5.0 mg/mL, dissolved in distilled water) were added into a 50 mL centrifuge tube, followed by shaking at 250 rpm at 37 $^{\circ}\text{C}$ for different adsorption time (10, 20, 30, 40, 50, 60, 70 and 80 min). After centrifuging at $3600 \times g$ for 5 min, the $D_{cr}\%$, $D_{pr}\%$ and $R_{rr}\%$ of the supernatant was determined according to the above method. And deproteinization and decolorization efficiency depend on the value of ξ .

Concentration of solution

Two g of pretreated optimized resin and 20 mL of crude polysaccharide solution with different concentrations of 1.0, 3.0, 5.0, 7.0, 9.0 and 12 mg/mL dissolved in distilled water were added into a 50 mL centrifuge tube, and then executed in the same procedure as resin types test.

Initial pH of AvPs solution

Two g of pretreated optimized resin and 20 mL of crude polysaccharide solution with the optimized concentration dissolved in water with different pH values of 4.0, 5.0, 6.0, 7.0, 8.0, 9.0 and 10.0 were added into a 50 mL centrifuge tube, and then executed in the same procedure as resin types test.

2.6 Optimization of flow rate by dynamic adsorption

Pretreated optimized resin was packed in a lab scale glass column (30 \times 120 mm) where the dynamic adsorption experiments were carried out. The resin column was flushed thoroughly with deionized water of 5 BV. The optimized concentration solution of AvPs dissolved in water with optimized pH value was loaded onto the resin column with a constant flow velocity of 1, 1.5, 2.0, 3.0 BV/h. For each flow velocity, the column was reloaded using new resin. The effluent (5 mL/tube) was collected by auto-partial collector (BS-100A Shanghai Huxi Instrument Equipment Co., Ltd, Shanghai, China). The $D_{cr}\%$, $D_{pr}\%$ and $R_{rr}\%$ in the effluence were detected by the same method mentioned above, and the value of ξ was calculated mentioned above.

2.7 Characterization of AvPs before and after adsorption

$D_{cr}\%$, $D_{pr}\%$ and $R_{rr}\%$ of AvPs before and after adsorption were determined using the method mentioned above. Then, molecular weight distribution, the monosaccharide composition, conformation structure, and the characteristics of ultraviolet (UV) /vis spectroscopy, Fourier-transform infrared (FT-IR) spectra, ^1H -nuclear magnetic resonance spectroscopy (^1H NMR) and Congo-red analysis were tested to reveal whether structure characteristics changes was happened during the resin adsorption process.

Molecular weight distribution analysis

The polysaccharide molecular weight distribution was estimated by high-performance gel permeation chromatography (HPGPC) (Liu et al., 2015). The HPGPC instrument was equipped with a Daojing LC-20AT HPLC system (Shimadzu, Kyoto, Japan), TSK-gel GMPW_{xl} column (7.8 mm \times 30 cm) and ELSD detector (Alltech, Deerfield, Illinois, USA). The temperature of the detector drift tube and the nitrogen pressure were set to 115 $^{\circ}\text{C}$ and 350 kPa, respectively. The sample injection volume was 10 μL . The column was calibrated with deionized water as the mobile phase at a rate of 0.7 mL/min. The sample was then eluted with deionized water as the mobile phase at the same rate.

Ultraviolet analysis

UV/vis full-wave spectra (230-800 nm) and FT-IR (400-4000 cm^{-1}) of the samples were measured respectively by UV/vis spectrophotometer mentioned above.

Monosaccharide composition analysis

The monosaccharide composition was analyzed using the method of Pan et al. (2018), with minor modifications. The polysaccharide (approximately 3.0 mg) was hydrolyzed in 0.5 mL of 3 M trifluoroacetic acid (TFA) at 90 $^{\circ}\text{C}$ for 6 h in a sealed 10-mL

ampoule filled with N₂. The sample was then cooled, transferred to a 1.5-mL Eppendorf (EP) tube, and centrifuged at 12000 × g for 2 min. The excess acid in the supernatant was completely removed by co-distillation with methanol. The hydrolysis products were dissolved in 0.3 M aqueous NaOH (400 μL) and derivatized with PMP (1-phenyl-3-methyl-5-pyrazolone, 200 μL) to improve UV absorption. After incubation at 70 °C for 1 h, the solution was cooled to room temperature and neutralized with 400 μL of 0.3 M HCl. The resulting solution was extracted with 1:1 (v/v) chloroform 3-4 times. The aqueous layer was collected and passed through a 0.22 μm membrane for HPLC analysis. An Agilent 1260 series instrument (Agilent, USA) equipped with a Xtimate® C18 column (250×4.6 mm i.d., 5 μm, Welch Materials Inc., Shanghai, China) was used. The derivatives were eluted with a mobile phase of water with acetonitrile (A), 0.01M PBS (pH7.2) (B) at a flow-rate of 1.0 mL/min with the following gradient program: 0-22 min, linear gradient 18-18% A (v/v, similarly hereinafter); 22-30 min, 20-30% A. The eluent was monitored at 245 nm. The injection volume was 10 μL.

FT-IR analysis.

FT-IR spectroscopy was performed using a Varian 1000 FT-IR spectrometer (Scimitar series, Varian Inc., USA). The polysaccharide was analyzed using the KBr disc method in the range of 4000-400 cm⁻¹.

¹H NMR analysis

The polysaccharide sample (approximately 20 mg) was dissolved in 0.6 mL D₂O for ¹H NMR analysis. Spectra were recorded at room temperature on Agilent-400 M spectrometer (Agilent, USA). The spectrograms were processed and analyzed using the MestReNova® software (Mestrelab Research Inc.)

Conformation structure

The conformation structure of AvPs was analyzed using the Congo-red method as described by Pan et al. (2018).

2.8 Partial biological activities of AvPs before and after adsorption

Total antioxidant capacity

Total antioxidant capacity of AvPs before and after treatment was determined using the improved ABTS method proposed by Tao et al. (2016) with a few modifications. ABTS radical solution (100 μL) was added to different AvPs concentrations (3.000, 1.500, 0.750, 0.375, 0.188, 0.094 and 0.047 mg/mL), and incubated for 10 min at 25 °C. Butylhydroxytoluene (BHT) was used as the positive antioxidant. The Abs was measured against a water blank at 734 nm. The antioxidant capacity was calculated using the following formula in Equation 5:

$$\text{ABTS radical cation inhibition (\%)} = \frac{1 - \text{Abs}_1}{\text{Abs}_0} \times 100\% \quad (5)$$

Where Abs₀ and Abs₁ were the Abs values of the ABTS radical solution in the absence of a sample and in the tested sample at

the end of the reaction, respectively. And the measurements were performed at least in triplicate.

Anticancer assays *in vitro*

Anticancer activity *in vitro* against SMMC-7721 and SK-Hep1 cell lines which were obtained from the Shanghai Genechem Co (Shanghai, China) was assessed using Sulforhodamine B (SRB) assay (Orellana & Kasinski, 2016). SMMC-7721 and SK-Hep1 cells were cultured in RPMI-1640 medium, supplemented with 10% fetal bovine serum (Gibco, Carlsbad, CA, USA), 1% penicillin and streptomycin (Invitrogen, Carlsbad, CA, USA) at 37 °C in an atmosphere of 5% CO₂. SMMC-7721 and SK-Hep1 cell lines from logarithmic growth phase (approximate 6000 cells/well in a sterile 96-well plate) were treated with AvPs (100 μL) before and after adsorption at different concentration (1.0, 2.0, 4.0 and 8.0 mg/mL), kept in an incubator (5% CO₂) at 37 °C for 48 h. After 48 h and removing the medium in the microtiter plates, assay was terminated by the addition of cold 10% TCA and incubated for 1 h at 4 °C, followed by removing the TCA solution by washing with deionized water for 5 times. After drying at room temperature, 100 μL 0.4% SRB was added to each of the wells and stood for 10 min at room temperature, followed by washing with 0.1% acetic acid solution to remove the SRB dye for 5 times which was not bound to cellular proteins, drying at room temperature, and dissolving at 100 μL 10 mM Tris buffer. The Abs was read on a plate reader at a wavelength of 530 nm. 100 μL medium replaced the AvPs solution was added to the test system as control. Tumor cell growth inhibition rate of SMMC-7721 and SK-Hep1 cell lines was calculated using the following formula in Equation 6:

$$\text{growth inhibition rate (\%)} = \frac{\text{OD}_C - \text{OD}_T}{\text{OD}_{T0}} \times 100\% \quad (6)$$

where OD_C, OD_{T0} and OD_T were the Abs values of the control, the tested sample at the beginning and end of cultivation, respectively. And the measurements were performed at least in triplicate.

2.9 Statistical analysis

All the results were expressed as the average ± standard deviation of triplicate determinations. An analysis of statistical significance was performed according to the one-way analysis of variance. Data analysis was performed with Microsoft Office Excel 2010 software or OriginPro 8 software.

3 Results and discussion

The yield of the AvPs extracted from *Actinidia valvata* Dunn roots was approximately 2.04%.

3.1 Selection of optimal absorption resin

There are many types of commercial macroporous resins. And the adsorption functions of resins are determined by surface adsorption, sieve classification, surface electrical property and hydrogen bonding interactions (Shi et al., 2017). Since the pigment and free protein are impurities which need to be removed from crude polysaccharide, and the polysaccharide

is the useful ingredient, which should have weak or no affinity with the resins. In order to screen optimal decoloration and deproteinization resin, 2 g of seven preprocessed resins (S-8, X-5, HP-20, AB-8, D101, HPD100, DM301) and 20 mL of 5 mg/mL AvPs solution (pH 7.0) were added to a 50 mL centrifuge tube. The AvPs solutions were shaken at 250 rpm at 37 °C for different time (10, 20, 30, 40, 50, 60, 70 and 80 min) by static adsorption experiments. As shown in Figure 1a and 1b, the decoloration ratio and deproteinization ratio for the tested resins were in the range of 15% to 30%, 25% to 50% in the adsorption time range of 10 to 80 min, respectively, while the recovery ratio of polysaccharide for the tested resins were almost more than 80% in the adsorption time range of 10 to 80 min in Figure 1c. Those results indicated that the tested resins showed moderated decoloration and deproteinization efficacy and a weak polysaccharide loss under the preliminary purification protocol. As the Figure 1d, although

the comprehensive adsorption effect index (ξ) of each resin changed over time, AB-8 and S-8 had significantly higher ξ value ($p > 0.05$) at most time points. Finally, macroporous resin S-8 was selected since it provided the highest absolute ξ value at a short time among all resins. Its ξ values were 61.91 ± 3.43 and 62.36 ± 1.95 at 40 and 50 min, respectively.

3.2 Selection of optimal initial concentration on resin AB-8

The initial concentration of AvPs affects the comprehensive adsorption effect index since the functional groups of resin have different adsorption efficiencies for pigment, protein and polysaccharide. Due to insufficient functional groups of the resin, the high initial concentration of AvPs mixed with the constant dosage of resin didn't completely adsorb pigments or proteins. Also, too low initial concentration of AvPs didn't increase the value of ξ . However, the adsorbable ingredients in the AvPs solution with a moderate initial concentration can be fully absorbed because of more functional groups of resins on the basis of the constant dosage of resins (Shi et al., 2017), thus it leads to a higher decoloration, deproteinization and a low recovery of polysaccharide. To optimize the proper initial concentration of AvPs, the static adsorption experiments with different initial concentration of AvPs (1, 3, 5, 7, 9 and 12 mg/mL) were performed. 2 g of AB-8 preprocessed resin and 20 mL of AvPs dissolved in deionized water were mixed and shaken at 250 rpm at 37 °C for 40 min. As shown in Figure 2a, resin AB-8 showed weak adsorption activity for the polysaccharide, and this could be the reason for adding less resin. The values of ξ showed a maximum value at the initial concentration of 3.0 mg/mL. The results suggested the initial concentration of 3.0 mg/mL should be used in following test.

3.3 Selection of optimal pH value on resin AB-8

The pH value determines the extent of ionization of adsorbed molecules (Al-Futaisi et al., 2007). And it was found in our preliminary experiments that pH affects the resin adsorption efficiency. Hence, the effects of pH values on the decoloration, deproteinization and recovery rate of polysaccharide were investigated. The static adsorption experiments with different initial pH value of AvPs at 3 mg/mL (pH = 4, 5, 6, 7, 8, 9, and 10) were performed. And the other parameters were the same as above. As shown in Figure 2b, too low pH was beneficial to remove pigments and proteins, but it also reduced the recovery rate of polysaccharide; too high pH not only did not improve the efficiency of removing pigments and proteins, but also reduced the recovery rate of polysaccharide. The values of ξ showed a maximum value at the initial pH value of 7 in the Figure 2b, and suggested the initial pH value of 7 should be used in following test.

3.4 Selection of optimal flow rate of AvPs solution on resin AB-8

The process of adsorption involves the diffusion of adsorbate and the interaction between the adsorbate molecules and the resin, including hydrogen bonding, simple stacking, or hydrophobic interactions. Resins can easily adsorb the molecules due to their large surface area and highly porous structure (Allen et al., 2003; Liu et al., 2010). Proper flow rate can give a full adsorption to

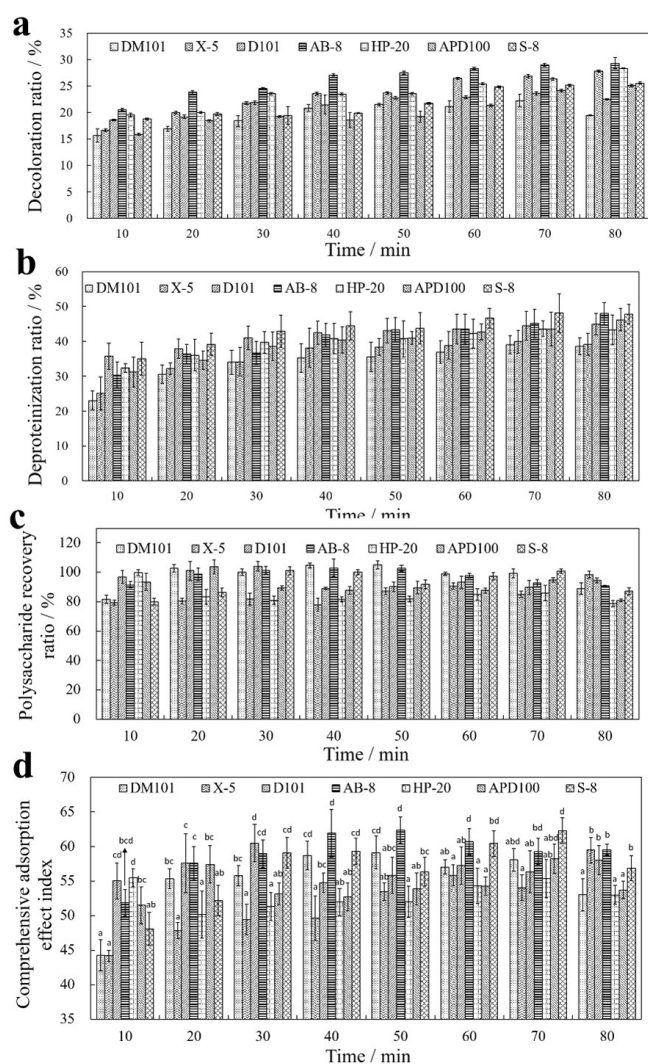


Figure 1. Comparison of decoloration ratios (a), deproteinization ratios (b), polysaccharide recovery ratios (c) and comparison of comprehensive adsorption effect index (ξ) (d) of AvPs using different resins for adsorption time (10-80 min). Values with different letters (a-f) are significantly different ($P < 0.05$) for the different resins at the same adsorption time.

Purification for polysaccharide using resin

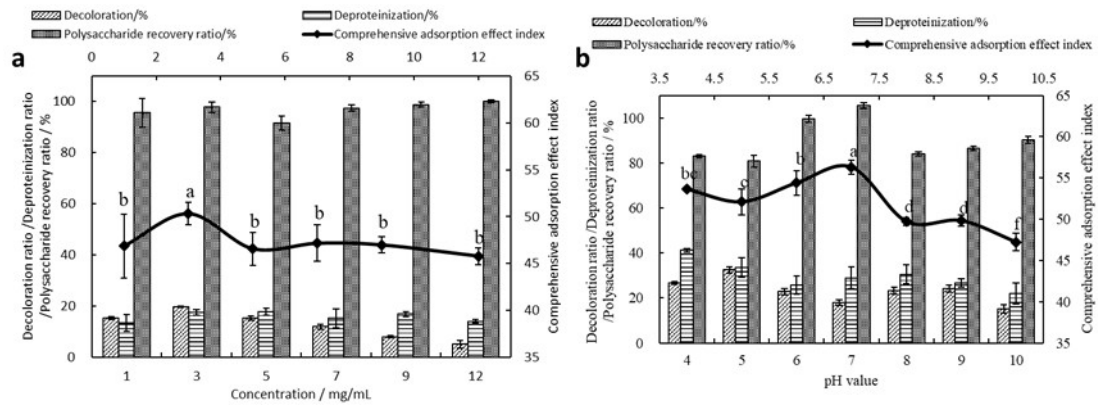


Figure 2. The effects of AvPs concentration (a), pH of the AvPs solution (b) on deproteinization, decolorization, polysaccharide recovery and comprehensive adsorption of resin AB-8 in static decoloration experiments.

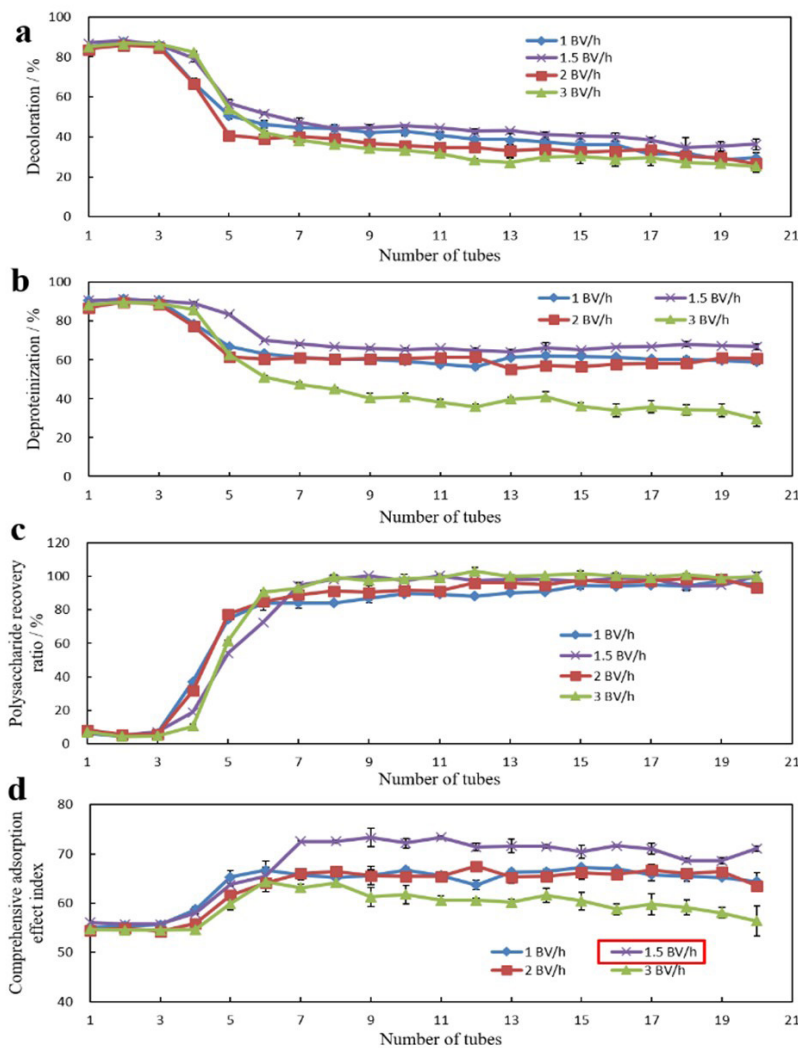


Figure 3. The effects of flow rate on deproteinization (a), decolorization (b), polysaccharide recovery (c) and comprehensive adsorption (d) of resin AB-8 column in dynamic adsorption experiment.

pigments or proteins, and a minimal loss of polysaccharides. In order to investigate the effect of flow rate on the decoloration, deproteinization and the recovery rate of polysaccharide, 100 mL of 3.0 mg/mL crude AvPs solution dissolved in deionized water

(pH 7.0) was loaded at different flow rate (1.0, 1.5, 2.0 and 3.0 BV/h) to a glass resin AB-8 column (3.0 × 12.0 cm). As shown in Figure 3, both the decoloration and deproteinization efficiency were the best, and the recovery rate of polysaccharide

was more than 95% after collecting the 7th tube. And the ξ values of samples at 1.5 BV/h were the highest than the others in Figure 3c. In addition, in the dynamic adsorption process, the loading solution first contacts the resin on the upper part of the column, the first reaches the saturated saturation state, and then this saturated adsorption state gradually moves down to form a chromatographic band. When adsorption reaches the breakthrough point, the adsorption stops. In order to investigate the breakthrough point, 500 mL of 3.0 mg/mL crude AvPs solution was loaded at the optimal flow rate of 1.5 BV/h on the same protocol as above. The decoloration and deproteinization ratios still kept relatively stable reached 5 BV. Therefore, 1.5 BV/h was selected as the optimal flow rate of AvPs solution on resin AB-8 in the following test.

3.5 Characterization of AvPs

Resin AB-8 significantly removed impurities in AvPs, while retained as much polysaccharides as possible. As shown in Figure 4a, the color of AvPs solution changed from brown to very pale yellow after resin AB-8 treatment, and based on the Abs at 420 nm, more than half of the pigment has been removed. Most proteins were also removed from the solution of AvPs using resin AB-8 treatment (Figure 4b). In addition, the total contents of polysaccharide increased by 18.75% after treatment of resin AB-8 (Figure 4c). This result showed that resin AB-8 not only had a weak affinity for the polysaccharide, but also increased the polysaccharide content by removing impurities. As shown in Figure 4d, no significant absorption at 260-280 nm was observed in the UV spectrum after the treatment of resin AB-8, and indicated that most of proteins were removed by this resin.

In order to further analyze whether the structural characterization changes during the resin treatment, HPGPC, FT-IR, PMP-HPLC-DAD and ¹H NMR were used in the present work. As shown in Figure 5a, there was no significant change on retention time (RT) base on the HPGPC chromatogram before and after adsorption, which suggested that no sugar chain was broken during resin AB-8 treatment. As shown in Figure 5b, the FT-IR spectroscopy characteristics before and after adsorption were almost the same, indicating that the characteristic groups of AvPs were adequately retained after resin AB-8 treatment. As shown in Figure 5c, the contents of the major monosaccharide before and after adsorption was unchanged, and mannose (RT, 9.7 min), galactose (RT, 23.9 min), arabinose (RT, 24.17 min) and fucose (RT, 28.00 min) were the major monosaccharide of AvPs in both samples before and after adsorption. As shown in Figure 5d, the proton nuclear magnetic resonance response signals before and after adsorption were similar, which also indicated there was no degradation during the resin AB-8 treatment. And one major signal (5.1 ppm, Figure 5d) indicates that the configurations of the AvPs pyranose residues were primarily the α -form (Pan et al., 2019). Based on the results of primary structure obtained above, the structural characteristics of AvPs remained unchanged using resin AB-8 adsorption.

The conformation structure of the sugar chain is not only affected by the primary structure, but also by the environment of the sugar chain. In order to define the 3D structure characteristics of AvPs during resin AB-8 treatment, Congo-red analysis was investigated, since Congo red can combine with helical polysaccharides, resulting in a large red shift of λ_{\max} (Deng et al., 2019; Shang et al., 2017), therefore, the shifts in the visible

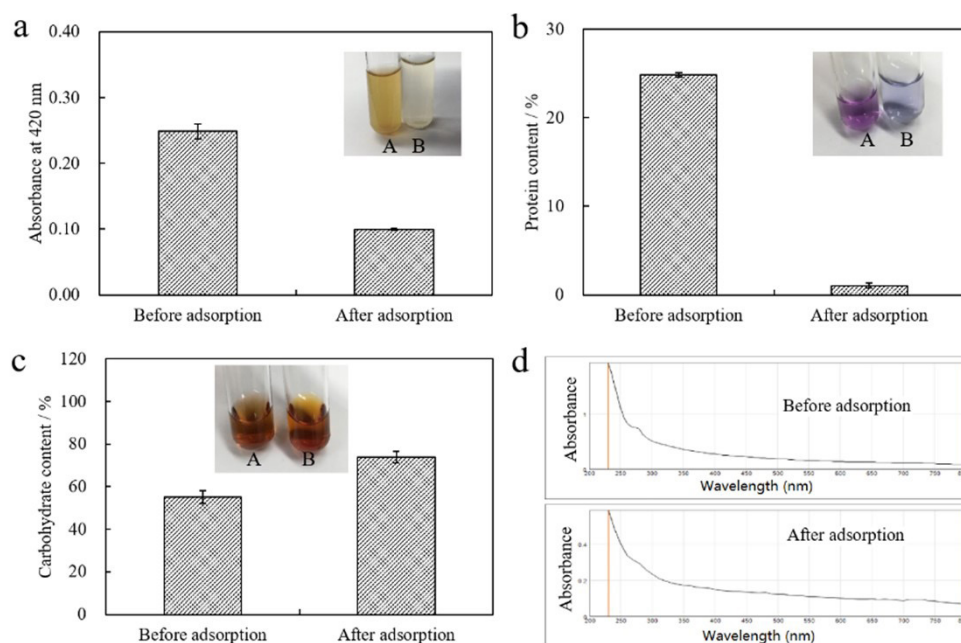


Figure 4. The absorbance at 420 nm (a), protein content (b), carbohydrate content (c) and UV-vis spectrogram (d) of AvPs solutions before and after adsorption by resin AB-8. A, the photograph of AvPs solutions before adsorption by resin AB-8; B, the photograph of AvPs solutions after adsorption by resin AB-8.

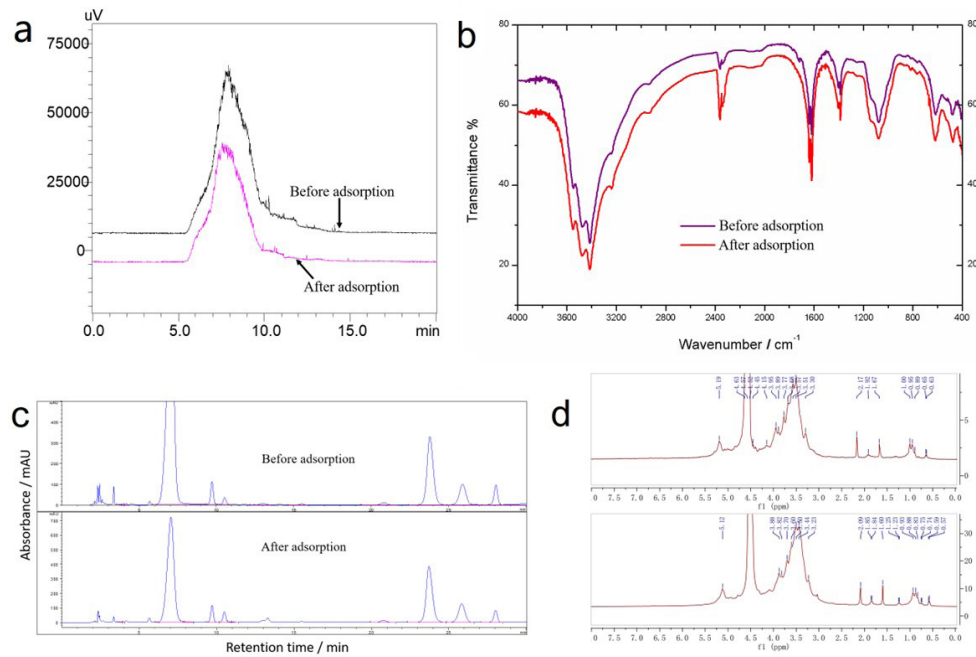


Figure 5. HPGPC chromatogram (a), FT-IR spectrogram (b), PMP-monosaccharide composition HPLC chromatogram (c) and ¹H NMR spectrum (d) of AvPs solutions before and after adsorption by resin AB-8.

maximum absorption of the polysaccharide's complexes with Congo red recorded on a UV-Vis spectrophotometer could be the conformation structure of AvPs. As shown in Figure 6, The λ_{max} values of the polysaccharide AvPs-Congo red complexes before and after resin AB-8 adsorption at various NaOH concentrations of 0-0.5 M were similar, which suggested that AvPs held the triple-helix conformation structure by comparison with the Congo red solution, and that the triple-helix conformation structure was not destroyed during the resin AB-8 treatment.

Based on the results obtained above, the structural characteristics of AvPs remained unchanged, and suggested that resin AB-8 was a proper material to purification of crude AvPs.

3.6 Partial biological activities

Total antioxidant capacity

The total antioxidant capacity was determined by a modified version of the improved ABTS method proposed by Tao et al. (2016). As shown in Figure 7, the antioxidant activities of AvPs before and after adsorption showed obvious dose-response curves at the concentrations below 1.0 mg/mL, and all reached at 100% to ABTS radical scavenging ability at 1.5 mg/mL. This result indicated AvPs after adsorption still had good antioxidant activity. In addition, the antioxidant activity of AvPs before adsorption with the IC₅₀ value of 0.188 mg/mL was stronger than that of AvPs after adsorption with the IC₅₀ value of 0.370 mg/mL, and which might due to removing of some active impurities by resin AB-8. Although the antioxidant activity of the sample was reduced after adsorption, the activity did not change substantially, and the AvPs activity before and after adsorption was still strong compared to the positive control BHT.

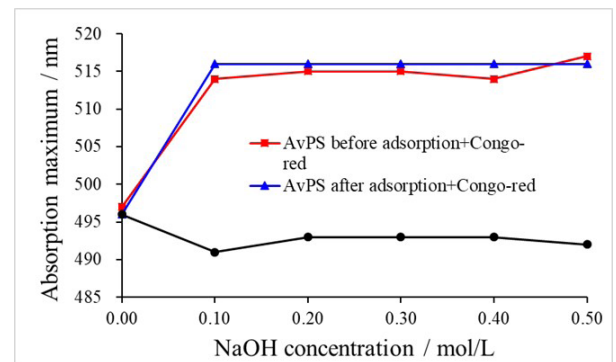


Figure 6. The maximum absorption wavelengths of AvPs -Congo red complexes before and after adsorption by resin AB-8 over the NaOH concentration range of 0-0.5 mol/L.

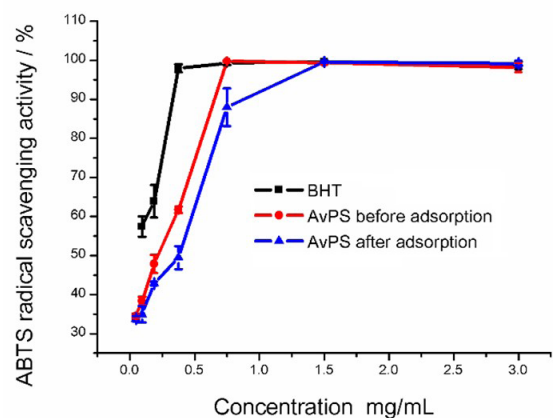


Figure 7. ABTS radical scavenging activity of AvPs before and after adsorption by resin AB-8 and the positive control (BHT).

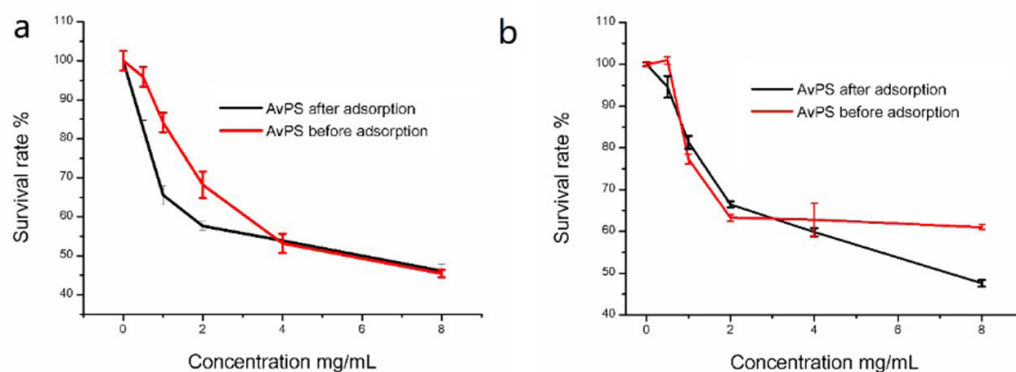


Figure 8. The survival rate of the SK-Hep1 (a) and SMMC-7721 (b) human hepatocellular carcinoma cells treated by AvPs before and after adsorption by resin AB-8.

Anticancer capacity

Liver cancer is one of the major threats to human health, and currently common chemotherapeutic drugs have great toxic and side effects (Sullivan et al., 2018). Some polysaccharides, as low-toxic macromolecular compounds, show good antitumor activity (Carnachan et al., 2019; Pan et al., 2019; Zheng et al., 2020). In the past report, low molecular weight compounds from *A. valvata* Dunn exhibited a good antitumor and anti-inflammatory activity (Xin et al., 2011). In the present report, anti-liver cancer activity was investigated by SRB assay against SMMC-7721 and SK-Hep1 cell lines. As shown in Figure 8, the AvPs before and after adsorption showed a good growth inhibitory activity *in vitro* to SMMC-7721 and SK-Hep1 cell lines, and the activity was similar. For example, the IC_{50} values of AvPs before and after adsorption were almost the same to SK-Hep1 (approximately 4.0 mg/mL). Those result suggested that the treatment of resin AB-8 to AvPs did not significantly lose its anti-liver cancer activity, and it also further confirmed that AvPs had the potential to further develop into an anti-liver cancer adjuvant.

4 Conclusion

Resin AB-8 showed a good comprehensive adsorption effect index to polysaccharide from the root of *Actinidia valvata* (AvPs) under the optimized parameter conditions as follows: a concentration of crude polysaccharide of 3 mg/mL, an adsorption time of 40 min, an initial pH of 7.0, a flow rate of 1.5 BV/h. The structural characteristics of AvPs remained unchanged after resin AB-8 adsorption. Moreover, AvPs can keep the stability of biological activity after the resin AB-8 treatment, and show obviously antioxidant and anticancer activities *in vitro* as well. This research suggests that this method is promising for the deproteinization and decolorization of AvPs which could be explored as a potential antioxidant or anticancer agent for use in functional food or medicine.

Conflict of interest

The authors declare no competing financial interests.

Acknowledgements

This work was supported by the Science and Technology Foundation of Guizhou Province (QKH20191346), the Science and

Technology Plan Project of Guizhou, China (QKPTRC2019035), the Science & Technology Talent Support Project of the Educational Department of Guizhou Province (KY 2018055), the innovation and Entrepreneurship Training Program for College Students of Zunyi Medical University (ZYDC2020101), and the Science and Technology Department of Zunyi city of Guizhou province of China (20207). We are grateful to the assistance of school of Pharmacy, Zunyi Medical University, Zunyi, China for providing FT-IR instrument and the help of Dr. Fangming, Lou and Dr. Fuming, Yuan in FT-IR and NMR assay, respectively.

References

- Agudo, J. A. G., Cubero, M. T. G., Benito, G. G., & Miranda, M. P. (2002). Removal of coloured compounds from sugar solutions by adsorption onto anionic resins: equilibrium and kinetic study. *Separation and Purification Technology*, 29(3), 199-205. [http://dx.doi.org/10.1016/S1383-5866\(02\)00083-7](http://dx.doi.org/10.1016/S1383-5866(02)00083-7).
- Al-Futaisi, A., Jamrah, A., & Al-Hanai, R. (2007). Aspects of cationic dye molecule adsorption to palygorskite. *Desalination*, 214(1-3), 327-342. <http://dx.doi.org/10.1016/j.desal.2006.10.024>.
- Allen, S. J., Gan, Q., Matthews, R., & Johnson, P. A. (2003). Comparison of optimised isotherm models for basic dye adsorption by kudzu. *Bioresource Technology*, 88(2), 143-152. [http://dx.doi.org/10.1016/S0960-8524\(02\)00281-X](http://dx.doi.org/10.1016/S0960-8524(02)00281-X). PMID:12576008.
- Braünlich, P. M., Inngjerdigen, K. T., Inngjerdigen, M., Johnson, Q., Paulsen, B. S., & Mabusela, W. (2018). Polysaccharides from the South African medicinal plant *Artemisia afra*: structure and activity studies. *Fitoterapia*, 124, 182-187. <http://dx.doi.org/10.1016/j.fitote.2017.11.016>. PMID:29155274.
- Carnachan, S. M., Bell, T. J., Hinkley, S. F., & Sims, I. M. (2019). Polysaccharides from New Zealand native plants: a review of their structure, properties, and potential applications. *Plants*, 8(6), 163. <http://dx.doi.org/10.3390/plants8060163>. PMID:31181819.
- Chen, X., Yuan, L., Du, J., Zhang, C., & Sun, H. (2019). The polysaccharide from the roots of *Actinidia eriantha* activates RAW264.7 macrophages via regulating microRNA expression. *International Journal of Biological Macromolecules*, 132, 203-212. <http://dx.doi.org/10.1016/j.ijbiomac.2019.03.158>. PMID:30914371.
- Deng, W., Yang, X., Zhu, Y., Yu, J., & Xu, X. (2019). Structural characterization and hypolipidemic activities of purified stigma maydis polysaccharides. *Food Science & Nutrition*, 7(8), 2674-2683. <http://dx.doi.org/10.1002/fsn3.1123>. PMID:31428354.

- Feng, Y. T., Chen, S. Y., Jiang, W. M., & Fu, C. X. (2004). Study on the effective components of *Actinidia macrosperma* (II)-Analysis on the amino acids. *Journal of Zhejiang University*, 30(2), 189-190.
- Huang, G., Shu, S., Cai, T., Liu, Y., & Xiao, F. (2012). Preparation and deproteinization of garlic polysaccharide. *International Journal of Food Sciences and Nutrition*, 63(6), 739-741. <http://dx.doi.org/10.3109/09637486.2011.652599>. PMID:22248003.
- Huang, Y., Zhu, Q., Ye, X., Zhang, H., & Peng, Y. (2021). Purification of polysaccharide from *Solanum nigrum* L. by S-8 macroporous resin adsorption. *Food Science and Technology*. Ahead of print. <http://dx.doi.org/10.1590/fst.68120>.
- Jamshidi-Kia, F., Lorigooini, Z., & Amini-Khoei, H. (2018). Medicinal plants: past history and future perspective. *Journal of Herbmed Pharmacology*, 7(1), 1-7. <http://dx.doi.org/10.15171/jhp.2018.01>.
- Jia, D., Zhang, J., Lan, R., Yang, H., & Sun, Y. (2013). A simple preparative method for isolation and purification of polysaccharides from mulberry (*Morus alba* L.) leaves. *International Journal of Food Science & Technology*, 48(6), 1275-1281. <http://dx.doi.org/10.1111/ijfs.12087>.
- Li, L., Xue, Y., Zhang, H., Liu, Y., Yi, F., & Dong, Y. (2020). A new polysaccharide isolated from *Dendrobium officinale*, stimulates aquaporin-3 expression in human keratinocytes. *Food Science and Technology*, 41(1), 90-95. <http://dx.doi.org/10.1590/fst.31119>.
- Li, X. J., Fu, Y. J., Luo, M., Wang, W., Zhang, L., Zhao, C. J., & Zu, Y. G. (2012). Preparative separation of dryofragin and aspidin BB from *Dryopteris fragrans* extracts by macroporous resin column chromatography. *Journal of Pharmaceutical and Biomedical Analysis*, 61, 199-206. <http://dx.doi.org/10.1016/j.jpba.2011.12.003>. PMID:22209481.
- Liang, L., Liu, G., Yu, G., Song, Y., & Li, Q. (2019). Simultaneous decoloration and purification of crude oligosaccharides from pumpkin (*Cucurbita moschata* Duch) by macroporous adsorbent resin. *Food Chemistry*, 277, 744-752. <http://dx.doi.org/10.1016/j.foodchem.2018.10.138>. PMID:30502211.
- Liu, J., Luo, J., Sun, Y., Ye, H., Lu, Z., & Zeng, X. (2010). A simple method for the simultaneous decoloration and deproteinization of crude levan extract from *Paenibacillus polymyxa* EJS-3 by macroporous resin. *Bioresource Technology*, 101(15), 6077-6083. <http://dx.doi.org/10.1016/j.biortech.2010.03.019>. PMID:20346649.
- Liu, L., Lu, Y., Li, X., Zhou, L., Yang, D., Wang, L., & Chen, Y. (2015). A novel process for isolation and purification of the bioactive polysaccharide TLH-3' from *Tricholoma lobayense*. *Process Biochemistry*, 50(7), 1146-1151. <http://dx.doi.org/10.1016/j.procbio.2015.04.011>.
- Liu, Y., & Li, S. M. (2020). Extraction optimization and antioxidant activity of *Phyllanthus urinaria* polysaccharides. *Food Science and Technology*, 41(Suppl. 1), 91-97. <http://dx.doi.org/10.1590/fst.11320>.
- Masuko, T., Minami, A., Iwasaki, N., Majima, T., Nishimura, S. L., & Lee, Y. C. (2005). Carbohydrate analysis by a phenol-sulfuric acid method in microplate format. *Analytical Biochemistry*, 339(1), 69-72. <http://dx.doi.org/10.1016/j.ab.2004.12.001>. PMID:15766712.
- Orellana, E. A., & Kasinski, A. L. (2016). Sulforhodamine B (SRB) assay in cell culture to investigate cell proliferation. *Bio-Protocol*, 6(21), e1984. <http://dx.doi.org/10.21769/BioProtoc.1984>. PMID:28573164.
- Pan, F., Hou, K., Li, D. D., Su, T. J., & Wu, W. (2019). Exopolysaccharides from the fungal endophytic *Fusarium* sp. A14 isolated from *Fritillaria unibracteata* Hsiao et KC Hsia and their antioxidant and antiproliferation effects. *Journal of Bioscience and Bioengineering*, 127(2), 231-240. <http://dx.doi.org/10.1016/j.jbiosc.2018.07.023>. PMID:30177486.
- Pan, F., Su, T. J., Liu, Y., Hou, K., Chen, C., & Wu, W. (2018). Extraction, purification and antioxidation of a polysaccharide from *Fritillaria unibracteata* var. *wabuensis*. *International Journal of Biological Macromolecules*, 112, 1073-1083. <http://dx.doi.org/10.1016/j.ijbiomac.2018.02.070>. PMID:29447973.
- Sevag, M., Lackman, D., & Smolens, J. (1938). The isolation of the components of streptococcal nucleoproteins in serologically active form. *The Journal of Biological Chemistry*, 124(2), 425-436. [http://dx.doi.org/10.1016/S0021-9258\(18\)74048-9](http://dx.doi.org/10.1016/S0021-9258(18)74048-9).
- Shang, H. M., Zhou, H. Z., Li, R., Duan, M. Y., Wu, H. X., & Lou, Y. J. (2017). Extraction optimization and influences of drying methods on antioxidant activities of polysaccharide from cup plant (*Silphium perfoliatum* L.). *PLoS One*, 12(8), e0183001. <http://dx.doi.org/10.1371/journal.pone.0183001>. PMID:28837625.
- Shi, Y., Liu, T., Han, Y., Zhu, X., Zhao, X., Ma, X., Jiang, D., & Zhang, Q. (2017). An efficient method for decoloration of polysaccharides from the sprouts of *Toona sinensis* (A. Juss.) Roem by anion exchange macroporous resins. *Food Chemistry*, 217, 461-468. <http://dx.doi.org/10.1016/j.foodchem.2016.08.079>. PMID:27664659.
- Shi, Y., Yuan, Z., Xu, T., Qu, R., Yuan, J., Cai, F., Wang, Y., & Wang, X. (2019). An environmentally friendly deproteinization and decolorization method for polysaccharides of *Typha angustifolia* based on a metal ion-chelating resin adsorption. *Industrial Crops and Products*, 134, 160-167. <http://dx.doi.org/10.1016/j.indcrop.2019.03.054>.
- Sullivan, K. M., Kenerson, H. L., Pillarisetty, V. G., Riehle, K. J., & Yeung, R. S. (2018). Precision oncology in liver cancer. *Annals of Translational Medicine*, 6(14), 285. <http://dx.doi.org/10.21037/atm.2018.06.14>. PMID:30105235.
- Sun, H., Zhang, J., Chen, F., Chen, X., Zhou, Z., & Wang, H. (2015). Activation of RAW264. 7 macrophages by the polysaccharide from the roots of *Actinidia eriantha* and its molecular mechanisms. *Carbohydrate Polymers*, 121, 388-402. <http://dx.doi.org/10.1016/j.carbpol.2014.12.023>. PMID:25659714.
- Tao, Y., Wang, P., Wang, Y., Kadam, S. U., Han, Y., Wang, J., & Zhou, J. (2016). Power ultrasound as a pretreatment to convective drying of mulberry (*Morus alba* L.) leaves: Impact on drying kinetics and selected quality properties. *Ultrasonics Sonochemistry*, 31, 310-318. <http://dx.doi.org/10.1016/j.ulsonch.2016.01.012>. PMID:26964954.
- Walker, J. M. (2009). The bicinchoninic acid (BCA) assay for protein quantitation. In J. M. Walker (Ed.), *The protein protocols handbook* (pp. 11-15). Totowa: Humana Press.
- Wang, Q., Xu, Y., Gao, Y., & Wang, Q. (2018). *Actinidia chinensis* planch polysaccharide protects against hypoxia-induced apoptosis of cardiomyocytes in vitro. *Molecular Medicine Reports*, 18(1), 193-201. PMID:29750308.
- Wang, Q., Ying, T., Jahangir, M. M., & Jiang, T. (2012). Study on removal of coloured impurity in soybean oligosaccharides extracted from sweet slurry by adsorption resins. *Journal of Food Engineering*, 111(2), 386-393. <http://dx.doi.org/10.1016/j.jfoodeng.2012.02.005>.
- Wang, Z., Song, Y., & Hu, J. (2005). Morphological identification and the clinical application of the roots of *Actinidia chinensis* and *Actinidia valvata*. *Pharmaceutical Care and Research*, 5(2), 134.
- Xiao, X., Sun, R., Jiang, S., Du, T., Yang, G., & Ye, F. (2014). Progress of research on pharmacological action and clinical application for the root of Kiwifruit. *China Medical Herald*, 23, 157-159.
- Xie, J. H., Shen, M. Y., Nie, S. P., Li, C., & Xie, M. Y. (2011). Decolorization of polysaccharides solution from *Cyclocarya paliurus* (Batal.) Iljinskaja using ultrasound/H₂O₂ process. *Carbohydrate Polymers*, 84(1), 255-261. <http://dx.doi.org/10.1016/j.carbpol.2010.11.030>.
- Xin, H. L., Wu, Y. C., Su, Y. H., Sheng, J. Y., & Ling, C. Q. (2011). Novel flavonoids from the leaves of *Actinidia valvata* Dunn: structural

- elucidation and antioxidant activity. *Planta Medica*, 77(1), 70-73. <http://dx.doi.org/10.1055/s-0030-1250113>. PMID:20665371.
- Xin, H. L., Yue, X. Q., Xu, Y. F., Wu, Y. C., Zhang, Y. N., Wang, Y. Z., & Ling, C. Q. (2008). Two new polyoxygenated triterpenoids from *Actinidia valvata*. *Helvetica Chimica Acta*, 91(3), 575-580. <http://dx.doi.org/10.1002/hlca.200890060>.
- Xing, X., Cui, S. W., Nie, S., Phillips, G. O., Goff, H. D., & Wang, Q. (2013). A review of isolation process, structural characteristics, and bioactivities of water-soluble polysaccharides from *Dendrobium* plants. *Bioactive Carbohydrates and Dietary Fibre*, 1(2), 131-147. <http://dx.doi.org/10.1016/j.bcdf.2013.04.001>.
- Xu, Y., Ge, R., Du, J., Xin, H., Yi, T., Sheng, J., Wang, Y., & Ling, C. (2009). Corosolic acid induces apoptosis through mitochondrial pathway and caspases activation in human cervix adenocarcinoma HeLa cells. *Cancer Letters*, 284(2), 229-237. <http://dx.doi.org/10.1016/j.canlet.2009.04.028>. PMID:19457606.
- Yang, R., Meng, D., Song, Y., Li, J., Zhang, Y., Hu, X., Ni, Y., & Li, Q. (2012). Simultaneous decoloration and deproteinization of crude polysaccharide from pumpkin residues by cross-linked polystyrene macroporous resin. *Journal of Agricultural and Food Chemistry*, 60(34), 8450-8456. <http://dx.doi.org/10.1021/jf3031315>. PMID:22860708.
- Yu, Y., Shen, M., Song, Q., & Xie, J. (2018). Biological activities and pharmaceutical applications of polysaccharide from natural resources: a review. *Carbohydrate Polymers*, 183, 91-101. <http://dx.doi.org/10.1016/j.carbpol.2017.12.009>. PMID:29352896.
- Zhang, Y., Liu, L., & Ling, C. (2006). Inhibition effect of active fraction from *Actinidia valvata* on growth of transplanted mouse tumor cells and preliminary study of its mechanism. *Zhongguo Zhong Yao Za Zhi*, 31(11), 918-920. PMID:17048634.
- Zheng, H. G., Chen, J. C., Weng, M. J., Ahmad, I., & Zhou, C. Q. (2020). Structural characterization and bioactivities of a polysaccharide from the stalk residue of *Pleurotus eryngii*. *Food Science and Technology*, 40(Suppl 1), 235-241. <http://dx.doi.org/10.1590/fst.08619>.